Volume 4 | Number 12 | December 2020

MATERIALS CHEMISTRY

FRONTIERS

Themed issue: In celebration of Prof. Fred Wudl's 80th Birthday

CCS 中国化学会 CHINESE CHEMICAL SOCIETY
ICCAS
ROYAL SOCIETY OF CHEMISTRY
rsc.li/frontiers-materials

MATERIALS CHEMISTRY
FRONTIERS

RESEARCH ARTICLE

View Article Online
View Journal | View Issue

Cite this: *Mater. Chem. Front.*, 2020, **4**, 3521

Pressure-induced valence transition in the mixed-valence $(Sm_{1/3}Ca_{2/3})_{2.75}C_{60}$ fulleride†

Naoya Yoshikane,[a] Keisuke Matsui,[a] Takeshi Nakagawa,[b] Anastasia G. V. Terzidou,[c] Yasuhiro Takabayashi,[de] Hitoshi Yamaoka,[f] Nozomu Hiraoka,[g] Hirofumi Ishii,[g] John Arvanitidis[c] and Kosmas Prassides[*ad]

$(Sm_{1/3}Ca_{2/3})_{2.75}C_{60}$ is a member of the family of non-stoichiometric strongly-correlated rare-earth fullerides, $(Sm_{1-x}Ca_x)_{2.75}C_{60}$ ($0 \leq x \leq 1$), in which an orthorhombic $2 \times 2 \times 2$ supercell of the face-centred cubic (fcc) unit cell of stoichiometric A_3C_{60} (A = alkali metal) fullerides is stabilized by the long-range ordering of partially-occupied metal sites. At ambient temperature and pressure, it is a mixed valence compound with an average Sm valence of +2.33(2) implying a formal charge of −5.78 for the C_{60} anions. Here we study its electronic response to the application of pressure in the range 0–9 GPa. Synchrotron X-ray absorption measurements in the high-resolution partial fluorescence yield mode (PFY-XAS) at ambient temperature show the onset of an abrupt strongly hysteretic (width ∼2.5 GPa) first-order reversible phase transition at ∼4 GPa, accompanied by a drastic increase in the bulk Sm valence by ∼20% to +2.71(3). This is coincident with the huge lattice contraction and concomitant insulator-to-metal transition encountered before for $Sm_{2.75}C_{60}$ in the same pressure range and provides a possible explanation of the physical properties in terms of the strong coupling between the lattice and electronic degrees of freedom. The behaviour is reminiscent of the electronic and lattice response to pressure of highly correlated Kondo insulators like SmS and its ternary derivatives, $Sm_{1-x}R_xS$ (R = Ca, Y, *etc.*). However, a distinguishing feature of the fulleride systems is that the C_{60} anionic sublattice can act as an electron reservoir due to the availability of a close-lying band derived by the t_{1g} orbitals and can accept excess charge as the 4f-electron occupation number decreases. The observed electronic response as a function of pressure is thus opening new possibilities for accessing metallic fullerides at elevated pressures.

Received 14th September 2020,
Accepted 15th October 2020

DOI: 10.1039/d0qm00707b

rsc.li/frontiers-materials

1. Introduction

Rare-earth (RE) metal C_{60} fullerides constitute an intriguing class of strongly-correlated molecular systems[1] as they present the possibility of strong coupling between two electronically active sublattices, the anionic $p\pi(C_{60})$ and cationic 4f,5d(RE) sublattices both of which are dominated by strong electronic correlations.[2,3] To date, metal fulleride research has been dominated by work on alkali fullerides, especially those with stoichiometry A_3C_{60} (A = alkali metal). These have emerged as archetypal strongly correlated systems with superconducting transition temperatures, T_c as high as 38 K[4] and upper critical magnetic fields, H_{c2} in excess of 90 T.[5] Nonetheless the electronic properties are entirely dominated by the narrow band behaviour of the C_{60} anion sublattice – the supporting cation sublattice is invariably electronically inactive and only plays a charge-balancing role as a structural spacer.[6] A comparable but exactly reverse situation is encountered in rare earth compounds which represent one of the most fascinating classes of strongly correlated systems that include Kondo insulators and heavy fermions.[7,8] Here the properties are dominated by the extreme narrow-band behaviour of the rare-earth cation f-electron sublattice with the supporting anion sublattice again playing a charge-balancing structural-spacer role. As electronically active anion solids, the rare-earth fullerides can have properties intrinsically distinct from comparable rare-earth compounds with closed shell anions, and the emergence

[a] *Department of Materials Science, Graduate School of Engineering, Osaka Prefecture University, Osaka 599-8531, Japan. E-mail: k.prassides@mtr.osakafu-u.ac.jp; Tel: +81 72 254 6162*
[b] *Center for High-Pressure Science & Technology Advanced Research, 100094 Beijing, P. R. China*
[c] *Physics Department, Aristotle University of Thessaloniki, 54124 Thessaloniki, Greece*
[d] *WPI-Advanced Institute for Materials Research (WPI-AIMR), Tohoku University, Sendai 980-8577, Japan*
[e] *Department of Physical Science and Engineering, Nagoya Institute of Technology, Nagoya 466-8555, Japan*
[f] *RIKEN SPring-8 Center, Sayo, Hyogo 679-5148, Japan*
[g] *National Synchrotron Radiation Research Center, Hsinchu 30076, Taiwan*

† Electronic supplementary information (ESI) available: Pressure dependence of the energies and intensities of the subpeaks used in the fitting of the experimental PFY-XAS spectra of $Sm_{1/3}Ca_{2/3}C_{60}$. See DOI: 10.1039/d0qm00707b

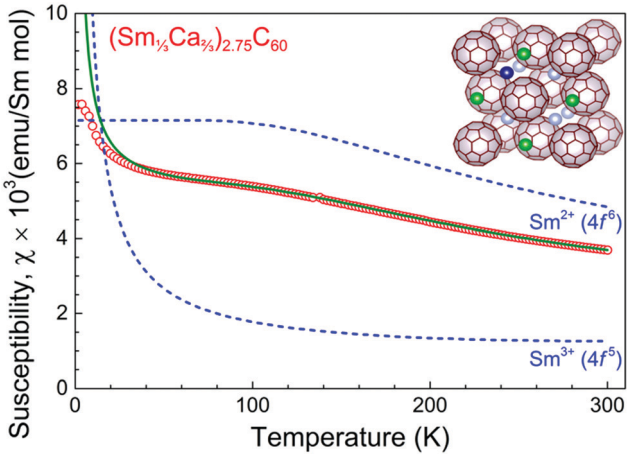

Fig. 1 Temperature dependence of magnetic susceptibilities. Open red circles show the total susceptibility of $(Sm_{1/3}Ca_{2/3})_{2.75}C_{60}$, obtained after subtracting the diamagnetic core contributions from the difference of the values measured at 4 and 2 T magnetic fields. The calculated magnetic susceptibilities (blue dashed lines) of the free Sm^{2+} and Sm^{3+} ions are also included. The susceptibility of Sm^{2+} ($4f^6$, $^7F_0$) is obtained by using van Vleck's formula which takes into account the presence of a J = 1 excited state at 420 K above the J = 0 ground state. For Sm^{3+} ($4f^5$, $^6H_{5/2}$), the susceptibility is calculated by considering the sum of the corresponding Curie and van Vleck contributions – in the latter case, the energy difference between the J = 5/2 ground and J = 7/2 excited state is 348 K. The green solid line through the experimental data is the weighted average of the susceptibility calculated assuming 0.68 and 0.32 contributions from Sm^{2+} and Sm^{3+}, respectively. The inset shows the building block of the unit cell of the orthorhombic superstructure of the compound, formed by doubling the shown subcell along all three lattice directions. Green and light-grey spheres correspond to off-centred octahedral and tetrahedral (randomly distributed samarium/calcium) metal cations, respectively, while the dark-blue sphere represents the partially-occupied tetrahedral site.

of novel phenomena such as co-existence of Kondo f-electron behaviour with C_{60}-based $p\pi$-electron superconductivity may be anticipated.

Rare-earth fulleride phases are not widely available mainly because of the synthetic difficulties in affording phase-pure materials in a reproducible way. Of interest has been the preparation of Eu_6C_{60} and Eu_9C_{70} fullerides that led to the isolation of molecular ferromagnets, which exhibit conducting and giant magnetoresistive behaviour with significant $\pi(C_{60})$-f,d(Eu) orbital interactions modulating the magnetic exchange.[9–11] However, most of the research work on rare-earth fullerides has focused on materials with stoichiometry, $RE_{2.75}C_{60}$ (RE = Yb, Sm). These non-stoichiometric compounds crystallize with a $2a \times 2a \times 2a$ superstructure of the face-centred cubic (fcc) unit cell of A_3C_{60} alkali fullerides arising from the long-rage ordered arrangement of partially occupied tetrahedral interstices (Fig. 1 inset).[12,13] The $RE_{2.75}C_{60}$ unit cell comprises 32 C_{60} units and 88 RE atoms together with 8 RE partially occupied sites. Although early claims for superconductivity[12,14] in this family proved erroneous,[13,15,16] it was apparent from the presence of non-stoichiometry and deviation from the ideal "RE_3C_{60}" stoichiometry that these materials may be endowed with interesting electronic properties associated with mixed valence states of the RE ions, *i.e.* that the average RE valence should be greater than +2. Indeed, magnetic susceptibility data clearly indicated deviation of the RE valence from +2.[13,15]

As a result of these considerations, an important finding was then that both $Sm_{2.75}C_{60}$ and $Yb_{2.75}C_{60}$ were discovered to exhibit on cooling isosymmetric phase transitions that are accompanied by giant negative thermal expansion (NTE).[13,15] The origin of this isotropic lattice response was ascribed to a temperature-induced valence transition of the RE ions from $+(2+\varepsilon)$ towards $+(2+\varepsilon')$ with $\varepsilon' < \varepsilon$ and this interpretation was supported by synchrotron X-ray absorption measurements.[1] This effect is immediately reminiscent of the valence or configuration transitions established in typical RE-based Kondo insulators such as SmS.[17,18] The connection becomes even more prominent when the electronic properties are probed by the application of external pressure. For instance, SmS undergoes a pressure-induced abrupt catastrophic transition from a semiconducting black to a metallic gold phase that was rationalised phenomenologically by a valence fluctuation ($4f^n5d^0 \leftrightarrow 4f^{n-1}5d^1$) model. In a similar fashion, $Sm_{2.75}C_{60}$ undergoes a pressure-induced first-order phase transition, which is accompanied by a huge lattice collapse of $\sim$6% at $\sim$4 GPa and a change in colour to gold, implying a drastic change in the conducting properties.[19] Complementary Raman spectroscopic measurements in the same pressure range confirm the occurrence of the transition and support the emergence of metallic behaviour.[20] The analogy with the behaviour of the Sm chalcogenides makes the possibility that $Sm_{2.75}C_{60}$ undergoes a similar pressure-induced valence transition towards a state with an increased average Sm valence $+(2+\varepsilon'')$ with $\varepsilon'' > \varepsilon$ highly likely.

Isovalent or aliovalent cation substitutions have been extensively used in the past to control the electronic configurations of the rare-earth ions and tune the rare-earth exchange interactions, the Fermi level position and the lattice constant (chemical pressure) in mixed valence Kondo insulators such as SmS.[21] The ternary phase fields Sm–R–S (R = Y, Ce, Nd, Ca, *etc.*) are recently drawing much attention in order to bring the insulator-to-metal transition to ambient pressure and utilize the huge NTE that accompanies the valence transition by tuning its operational temperature range.[22–24] In the process, it is of particular importance to clarify the differences on the valence transition between controlling size (chemical or physical pressure) and doping (electronic structure).

In a similar fashion, we have initiated the study of the ternary fulleride phases, $(Sm_{1-x}Ca_x)_{2.75}C_{60}$ $(0 \le x \le 1)$ in an attempt to mimic chemically the effect of physical pressure on the valence transition of $Sm_{2.75}C_{60}$ by taking advantage of the robust divalent character of the smaller valence-precise Ca^{2+} cations.[25] We found that the $(Sm_{1-x}Ca_x)_{2.75}C_{60}$ $(0 \le x \le 1)$ family of materials obeys Vegard's law with the Sm and Ca metal ions randomly distributed in the available octahedral and tetrahedral interstitial sites.[25] They also adopt the same orthorhombic superstructure (space group *Pcab*) of the face-centred cubic unit cell of A_3C_{60} (A = alkali metal) fullerides

arising from the long-range ordering of tetrahedral partially-occupied vacancies (Fig. 1 inset) consistent with the stoichiometry of the materials.[25] Moreover X-ray absorption spectroscopy measurements in the partial fluorescence yield mode (PFY-XAS) at the Sm-L_3 edge have authenticated the mixed valence state of Sm across the whole series of $(Sm_{1-x}Ca_x)_{2.75}C_{60}$ compositions. In particular, it turns out that, at ambient conditions, chemical pressure sensitively tunes the 4f electron occupation number with the average Sm valence, ν increasing quasi-continuously by $>10\%$ as x increases from 0 (for $Sm_{2.75}C_{60}$, ν = +2.07(3)) to 2/3 (for $(Sm_{1/3}Ca_{2/3})_{2.75}C_{60}$, ν = +2.33(2)). At the same time, the C_{60} anion charge remains nearly invariant at ≈ -5.78.[25]

To date, there has been no direct study of the rare-earth electronic states in rare-earth fullerides at elevated pressures. Synchrotron X-ray powder diffraction[19] and Raman spectroscopy[20] agree on the occurrence of a hysteretic phase transition for $Sm_{2.75}C_{60}$ in the vicinity of 4 GPa with dramatic changes in both lattice size and electronic/conducting properties. Here, we directly address the issue of the evolution of the Sm electronic states with applied pressure by means of PFY-XAS spectroscopy at the Sm-L_3 edge. We chose to investigate the calcium co-doped $(Sm_{1/3}Ca_{2/3})_{2.75}C_{60}$ fulleride as this was found to incorporate Sm at the highest average valence, ν known for these systems at ambient pressure at +2.33(2).[25] We find that ν initially increases monotonically to $\sim$4 GPa whereupon an abrupt phase transformation sets in – this is accompanied by a rapid increase in ν to +2.71(3) at $\sim$6.5 GPa. The electronic changes are reversible upon the release of pressure and are characterized by a large hysteresis, signature of the first-order nature of the transformation. They provide a possible rationalization of the pressure-induced drastic changes in structural and optical properties of rare-earth fullerides that may be coupled with the extreme fragility of the rare-earth valence.

2. Results and discussion

$(Sm_{1/3}Ca_{2/3})_{2.75}C_{60}$ is a member of the $(Sm_{1-x}Ca_x)_{2.75}C_{60}$ ($0 \leq x \leq 1$) family of materials with x = 2/3. Fig. 1 shows the measured magnetic susceptibility, χ *vs.* temperature data for $(Sm_{1/3}Ca_{2/3})_{2.75}C_{60}$, along with those calculated for the free Sm^{2+} and Sm^{3+} ions. For Sm^{2+} ($4f^6$, $^7F_0$), there is only a van Vleck contribution to the magnetic susceptibility, originating from the mixing of the J = 0 ground and the J = 1 excited state. On the other hand, the calculated susceptibility of Sm^{3+} ($4f^5$, $^6H_{5/2}$) is

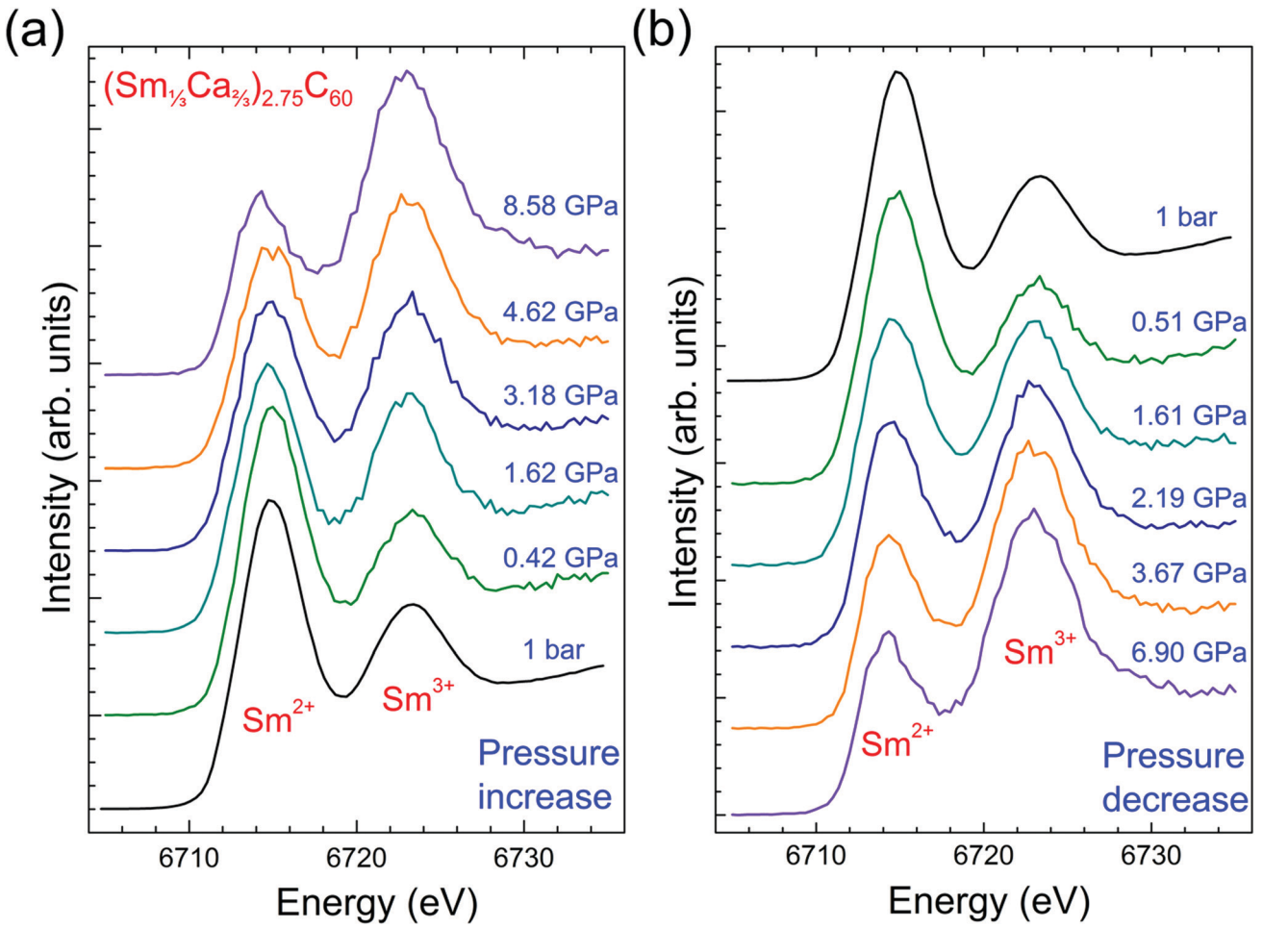

Fig. 2 Representative ambient-temperature Sm-L_3 edge PFY-XAS spectra of $(Sm_{1/3}Ca_{2/3})_{2.75}C_{60}$ at various pressures shown in linear scale, recorded upon pressure (a) increase and (b) decrease. The spectrum recorded at ambient conditions is also included in both panels.

derived by summing the corresponding Curie and van Vleck (mixing of the J = 5/2 ground and J = 7/2 excited states) contributions.[13] In mixed valence Sm-based compounds, an estimate of the average samarium valence can be derived from the magnetic susceptibility data at sufficiently high temperatures as a linear combination of the contributions of the two distinct Sm^{2+} and Sm^{3+} valence states.[26] As it can be inferred from Fig. 1, the experimental values of the susceptibility of $(Sm_{1/3}Ca_{2/3})_{2.75}C_{60}$ at high temperatures fall between those calculated for the two ionic states, in accord with the mixed valence character of samarium in this material. The experimental data can be reproduced well down to ~50 K (below which valence transitions are expected)[13,15] assuming 0.68 and 0.32 contributions from Sm^{2+} and Sm^{3+}, respectively (solid line through the data). These values lead to an estimate of the average samarium valence, ν of +2.32 in excellent agreement with that obtained directly by PFY-XAS measurements at ambient conditions (+2.33(2)) for the same composition.[25]

The PFY-XAS spectra of $(Sm_{1/3}Ca_{2/3})_{2.75}C_{60}$ at the Sm-L_3 edge at various pressures are displayed in Fig. 2 together with that measured under ambient conditions. We note that, since only one quantum transition (an intermediate state belonging to a shallow level) is selected in this X-ray spectroscopic technique, the lifetime broadening of the spectra (mainly originating from the deep core-hole in the final state) is suppressed, leading to a much better resolution than typical XAS measurements.[27] Compared to the ambient pressure spectrum in which the sample was contained in a glass capillary,[25] the sample chamber of the Be gasket in the present high pressure experiments is significantly more transparent to the synchrotron X-ray beam in the incident photon energy range used. This introduces the danger of causing radiation damage to the soft fulleride solids by X-ray illumination in the course of the measurements. Therefore, in order to avoid the occurrence of sample degradation, the incident X-ray beam power was reduced by a factor of ~30 compared to that of the ambient pressure experiments by introducing appropriately thick aluminium foil filters. This unavoidably led to a worsening in the signal-to-noise ratio compared to that achieved at ambient pressure (Fig. 2).[25] Nonetheless, good data statistics and improved spectral resolution still allow us to follow the pressure evolution of the average samarium valence with sufficient accuracy.

The appearance of two peaks separated by ~8 eV in the spectra shown in Fig. 2 and corresponding to the 2p → 5d dipolar excitations for divalent (lower energy peak) and trivalent (higher energy peak) samarium, unambiguously

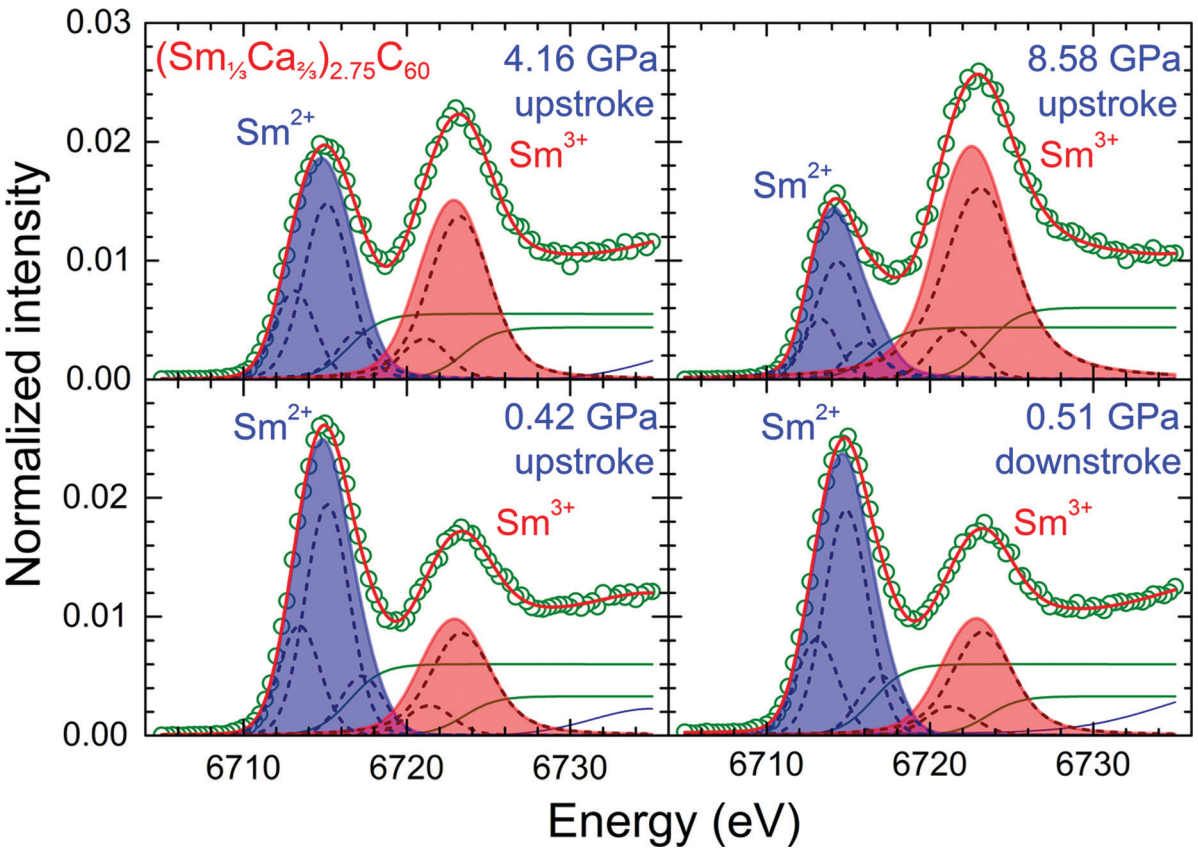

Fig. 3 Representative fits (solid lines through the experimental data) of the PFY-XAS spectra (open circles) of $(Sm_{1/3}Ca_{2/3})_{2.75}C_{60}$ recorded upon pressure increase (P = 0.42, 4.16 and 8.58 GPa, upstroke) and release (P = 0.51 GPa, downstroke). The two main peaks, corresponding to the 2p → 5d dipolar excitations for Sm^{2+} and Sm^{3+}, are represented as blue and red shaded areas, respectively. Solid green lines represent the arctangent functions used to describe the corresponding transitions to the continuum, while the solid blue line at the bottom is the underlying baseline. Dashed lines mark the Voigt components employed in the fitting procedure of the experimental data.

evidences the mixed valence character of the samarium ions in $(Sm_{1/3}Ca_{2/3})_{2.75}C_{60}$ at both ambient and elevated pressures.[28] At ambient and low pressures, the higher intensity of the Sm^{2+} peak compared to that of the Sm^{3+} one qualitatively indicates that the average samarium valence, ν is closer to +2 rather than +3. This situation is gradually altered with increasing pressure as the Sm^{3+} peak gains in intensity at the expense of that of Sm^{2+}, signalling a drastic decrease in the 4f electron occupation of the samarium ions induced by pressure. The reverse valence transition ($Sm^{3+} \rightarrow Sm^{2+}$) occurs upon pressure release. The transformation is reversible as the relative intensity of the two peaks in the spectrum recorded at 0.51 GPa upon depressurization is comparable to that in the spectra measured at ambient pressure and at 0.42 GPa at the start of the present measurements (Fig. 2a and b).

In order to extract quantitative information about the average valence, ν of samarium in $(Sm_{1/3}Ca_{2/3})_{2.75}C_{60}$ and its pressure dependence, the data were fitted by appropriate functions to account for the contributions of the Sm^{2+} and Sm^{3+} peaks together with that of the background. The fits of the PFY-XAS spectra at selected pressures recorded during the upstroke (P = 0.42, 4.16 and 8.58 GPa) and downstroke (P = 0.51 GPa) cycles are shown in Fig. 3. The spectral contribution attributed to Sm^{2+} was fitted by the sum of three Voigt functions (one main and two satellites) for the main peak and an arctangent-like function to account for the background originating from the corresponding transitions to the continuum. The need to use more than one Voigt function to satisfactorily reproduce each white peak originates from the crystal-field splitting of the Sm 5d band.[24,29] A similar fitting strategy was used for the Sm^{3+} spectral contribution except that it was found necessary to include only two Voigt functions to describe the corresponding main peak. In the lower pressure range of the experiments, an additional Voigt function was included in order to account for the small spectral uplift above 6730 eV (underlying baseline in Fig. 3). Fig. S1 and S2 (ESI†) collect together the pressure dependence of the energies and intensities of the individual subpeaks of the Sm^{2+} and Sm^{3+} components employed in the fits of the experimental PFY-XAS data. The average Sm valence, ν can be derived then from the relative integrated intensities of the divalent, $I(+2)$ and the trivalent, $I(+3)$ Sm PFY-XAS peaks (corresponding shaded areas in Fig. 3) by the expression: $\nu = 2 + \{I(+3)/[I(+2) + I(+3)]\}$.

The fit of the PFY-XAS spectrum at 0.42 GPa yields a value for the average samarium valence, ν = +2.31(3), similar to that obtained from the corresponding measurements on the same composition at ambient pressure (ν = +2.33(2)).[25] Such an agreement clearly demonstrates the reproducibility of our findings and confirms the successful loading of the highly air-/moisture-sensitive sample into the diamond anvil cell (DAC) for the high pressure experiments, completely avoiding any degradation. At the same time, the fit of the spectrum recorded at the highest pressure of our experiments (8.58 GPa), where the trivalent samarium peak clearly dominates, provides a value, ν = +2.71(3) for the average Sm valence – this corresponds to an increase of the Sm valence by 0.4 induced by pressure. Comparable changes associated with the pressure-induced transition from the semiconducting to the metallic phase have been reported for the Sm monochalcogenides, namely ~0.8 for SmS, ~0.6 for SmSe and ~0.5 for SmTe.[24]

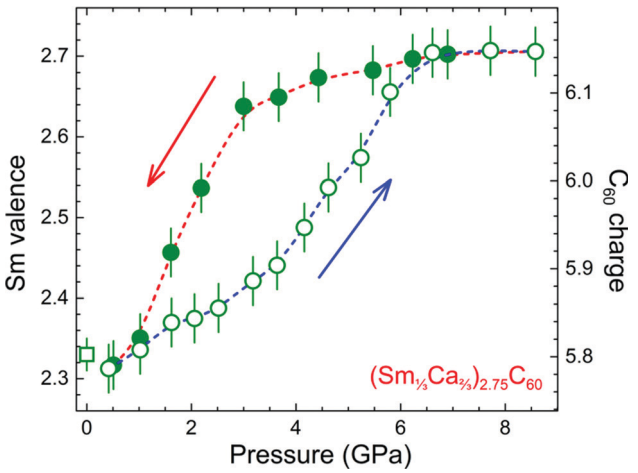

Fig. 4 Pressure dependence of the average samarium valence and C_{60} charge in $(Sm_{1/3}Ca_{2/3})_{2.75}C_{60}$. Open (solid) circles represent data obtained upon pressure increase (decrease), while the open square is the ambient pressure datum. Dashed lines through the data are guides to the eye.

The pressure dependence of ν in $(Sm_{1/3}Ca_{2/3})_{2.75}C_{60}$, as obtained from the fits of all the high pressure data recorded during the upstroke and downstroke cycles, is illustrated in Fig. 4. In the beginning, the valence increases slowly and continuously from +2.31(3) to +2.49(3) as the pressure approaches ~4 GPa. This is followed first by a pressure regime (~4–6.5 GPa) whereupon the average valence rapidly increases reaching a value of +2.71(3) and then by a plateau where ν remains invariant up to ~9 GPa, the highest pressure reached in the present measurements. On the other hand, upon pressure release, the average samarium valence is robust over a broad pressure range decreasing only very slightly to a value of +2.64(3) between 9 and 3 GPa. However, this is followed next by a rapid drop to +2.32(3) at 0.51 GPa (the lowest pressure achieved during depressurization), a value essentially identical to that measured at the beginning of the experiment at 0.42 GPa. The data confirm the reversible nature of the pressure-induced electronic changes and exclude any extraneous origin of the phase transformation as well as any sample degradation due to X-ray illumination. The large hysteretic behaviour – pressure width of the hysteresis loop is ~2.5 GPa – of the reversible $Sm^{2+} \leftrightarrow Sm^{3+}$ valence change (Fig. 4) is consistent with the transition being first-order in nature analogous to what is established for SmS.[30] Noticeably however, when compared with $Sm_{2.75}C_{60}$, the transition here appears to be more sluggish and the hysteretic loop significantly broader.

In $(Sm_{1/3}Ca_{2/3})_{2.75}C_{60}$, the abrupt Sm valence transition occurs over the range of 4 to 6.5 GPa upon pressurization. As both the lattice collapse and the insulator-to-metal transition evidenced for the binary $Sm_{2.75}C_{60}$ fulleride also occur over a comparable pressure range of 4–5 GPa,[19,20] the present results provide direct evidence for the strong coupling between the

charge and lattice degrees of freedom – both structural and conductivity changes are driven by changes in the electronic configuration possibly mediated by the C_{60} anionic sublattice.

The latter has the potential to act as a charge reservoir accepting electrons from the Sm 4f/5d bands in the course of the valence transition. The availability of the t_{1g}-derived C_{60} band, which can begin to be populated when the Sm valence exceeds values of 2.5–2.6 (Fig. 4) and the t_{1u}-derived C_{60} band is full, appears to be a crucial ingredient to allowing the valence change to proceed. Such an availability contrasts with the cases in which the anion sublattice comprises closed-shell anions like the chalcogenides.

Finally, given that the valence transition of samarium at elevated pressure is towards the generation of the magnetic Sm^{3+} ion with a $4f^5$:$^6H_{5/2}$ configuration also opens up the possibility of coupling to the magnetic degrees of freedom and the emergence of long-range magnetic ordering, in analogy with the Sm monochalcogenides in the high pressure golden phase.[31]

3. Conclusions

In summary, we have employed synchrotron X-ray spectroscopic (PFY-XAS) measurements to investigate the electronic properties of the mixed valence fulleride, $(Sm_{1/3}Ca_{2/3})_{2.75}C_{60}$ at elevated pressures. The observed pressure response of the average Sm valence, ν is similar to that of strongly correlated Kondo insulators such as SmS with a sharp decrease in the 4f-electron occupation number occurring abruptly above $\sim$4 GPa. The resulting $\sim$20% increase in ν to +2.71(3) coincides with the occurrence of a concomitant lattice collapse and the appearance of metallic behaviour in the same pressure range in the parent mixed valence fulleride, $Sm_{2.75}C_{60}$ providing a possible explanation of the observed properties, that may involve the strong coupling between lattice and electronic (valence) degrees of freedom. The availability of the t_{1g}-derived band of C_{60} appears crucial in being able to accommodate the excess charge generated by the pressure-induced $Sm^{2+} \rightarrow Sm^{3+}$ transition after the t_{1u}-derived band becomes fully occupied at $\nu \approx +2.55$ and drive the system to the metallic state. Therefore, given that the C_{60} sublattice can support superconductivity, the possibility emerges that mixed valence rare-earth fullerides can become superconducting at higher C_{60} doping levels achieved by further increase in the average rare-earth valence at elevated pressures, opening new prospects in this research field. Finally, the valence transition is reversible and of first-order as evidenced by its highly hysteretic behaviour together with the complete recovery of the electronic properties upon pressure release.

4. Experimental section

The $(Sm_{1/3}Ca_{2/3})_{2.75}C_{60}$ polycrystalline sample used in this work was prepared, chemically analyzed and structurally characterized, as reported elsewhere.[25] Due to the extreme sensitivity of the sample to air and moisture, all manipulations were undertaken in argon-filled gloveboxes ($H_2O/O_2 < 0.1$ ppm).

Ambient-pressure magnetic measurements were performed on a *ca.* 20 mg sample, sealed in a thin-walled quartz ampoule with a Quantum Design SQUID MPMS5 magnetometer. Temperature dependent magnetic susceptibility data were collected at 2 and 4 T under field-cooled protocols at temperatures between 1.8 and 300 K. The total susceptibilities were obtained after subtracting the diamagnetic core contributions from the difference of the values measured at applied magnetic fields of 4 and 2 T.

PFY-XAS spectra of $(Sm_{1/3}Ca_{2/3})_{2.75}C_{60}$ at the Sm-L_3 edge were collected at room temperature at the Taiwan BL12XU beamline, SPring-8, Japan, in a 90° geometry. For these experiments, the emitted photon energy was fixed around the maximum of the $L\alpha_1$ emission line at $\sim$5636 eV, while the incident photon energy was scanned across the Sm-L_3 edge.[32] For every individual spectrum, four different scans in the energy range 6735–6705 eV, divided into 90 energy steps with a measurement time of 5 s each, were averaged. The spectral intensity was normalized to the intensity recorded by a monitor situated before the DAC in which the sample was loaded. High pressure was generated by means of a 4-pin type DAC with a culet size of 700 μm, utilizing a 30 μm thick Be gasket with a 250 μm diameter hole at the centre. A pellet fragment of the sample was carefully placed in the sample chamber of the Be gasket, inside an Ar gas atmosphere glovebox in order to avoid sample oxidation. Daphne 7373 oil, which solidifies at 2.2 GPa at room temperature[33] was used as the pressure transmitting medium, while the pressure was calibrated by means of the ruby fluorescence method.[34]

Conflicts of interest

There are no conflicts to declare.

Acknowledgements

We thank SPring-8 for access to synchrotron X-ray facilities and Dr A Machida for the use of the glovebox at the facility. AGVT acknowledges the support by the Hellenic Foundation for Research and Innovation (HFRI) under the HFRI PhD Fellowship grant (Fellowship Number: 707). This work was financially supported by Grants-in-Aid for Scientific Research (JSPS KAKENHI Grant Numbers JP18H04303, JP18K18724, and JP19H04590) by the Ministry of Education, Culture, Sports, Science and Technology (MEXT), Japan, by the Murata Foundation and by the KAKENHI Specific Support Operation of Osaka Prefecture University. The experiments at the SPring-8 Taiwan beamline BL12XU were performed under SPring-8 Proposal No. 2017B4268, 2018B4252 and 2019A4264, corresponding to NSRRC Proposal No. 2018-1-058-1, 2018-1-058-3 and 2018-1-058-5, respectively.

Notes and references

1 K. Prassides, Y. Takabayashi and T. Nakagawa, Mixed valency in rare-earth fullerides, *Philos. Trans. R. Soc., A*, 2008, **366**, 151–161.

2 Y. Takabayashi and K. Prassides, Unconventional high-T_c superconductivity in fullerides, *Philos. Trans. R. Soc., A*, 2016, **374**, 20150320.

3 P. Wachter, Intermediate valence and heavy fermions, in *Handbook on the physics and chemistry of rare earths*, ed. K. A. Gschneidner, L. Eyring, G. H. Lander and G. R. Chopin, Elsevier Science B. V., Amsterdam, 1994, vol. 19, pp. 177–388.

4 Y. Takabayashi, A. Y. Ganin, P. Jeglic, D. Arcon, T. Takano, Y. Iwasa, Y. Ohishi, M. Takata, N. Takeshita, K. Prassides and M. J. Rosseinsky, The disorder-free non-BCS superconductor Cs_3C_{60} emerges from an antiferromagnetic insulator parent state, *Science*, 2009, **323**, 1585–1590.

5 Y. Kasahara, Y. Takeuchi, R. H. Zadik, Y. Takabayashi, R. H. Colman, R. D. McDonald, M. J. Rosseinsky, K. Prassides and Y. Iwasa, Upper critical field reaches 90 tesla near the Mott transition in fulleride superconductors, *Nat. Commun.*, 2017, **8**, 14467.

6 R. H. Zadik, Y. Takabayashi, G. Klupp, R. H. Colman, A. Y. Ganin, A. Potocnik, P. Jeglic, D. Arcon, P. Matus, K. Kamaras, Y. Kasahara, Y. Iwasa, A. N. Fitch, Y. Ohishi, G. Garbarino, K. Kato, M. J. Rosseinsky and K. Prassides, Optimized unconventional superconductivity in a molecular Jahn-Teller metal, *Sci. Adv.*, 2015, **1**, e1500059.

7 C. M. Varma, Mixed-valence compounds, *Rev. Mod. Phys.*, 1976, **48**, 219–238.

8 Q. Si and F. Steglich, Heavy fermions and quantum phase transitions, *Science*, 2010, **329**, 1161–1166.

9 K. Ishi, A. Fujiwara, H. Suematsu and Y. Kubozono, Ferromagnetism and giant magnetoresistance in the rare-earth fullerides $Eu_{6-x}Sr_xC_{60}$, *Phys. Rev. B: Condens. Matter Mater. Phys.*, 2002, **65**, 134431.

10 T. Takenobu, D. H. Chi, S. Margadonna, K. Prassides, Y. Kubozono, A. N. Fitch, K. Kato and Y. Iwasa, Synthesis, structure, and magnetic properties of the fullerene-based ferromagnets Eu_3C_{70} and Eu_9C_{70}, *J. Am. Chem. Soc.*, 2003, **125**, 1897–1904.

11 I. Margiolaki, S. Margadonna, K. Prassides, T. Hansen, K. Ishii and H. Suematsu, Magnetic structure of the europium fulleride ferromagnet Eu_6C_{60}, *J. Am. Chem. Soc.*, 2002, **124**, 11288–11289; J. Arvanitidis, D. Christofilos, G. A. Kourouklis, A. Paloumpi, K. Papagelis, S. Ves, Y. Iwasa and K. Prassides, Raman spectroscopic study of the rare-earth fullerides $Eu_{6-x}Sr_xC_{60}$, *Nanoscale*, 2011, **3**, 2490–2493.

12 E. Özdaş, A. R. Kortan, N. Kopylov, A. P. Ramirez, T. Siegrist, K. M. Rabe, H. E. Bair, S. Schuppler and P. H. Citrin, Superconductivity and cation-vacancy ordering in the rare-earth fulleride $Yb_{2.75}C_{60}$, *Nature*, 1995, **375**, 126–129.

13 J. Arvanitidis, K. Papagelis, S. Margadonna, K. Prassides and A. N. Fitch, Temperature-induced valence transition and associated lattice collapse in samarium fulleride, *Nature*, 2003, **425**, 599–602.

14 X. H. Chen and G. Roth, Superconductivity at 8 K in samarium-doped C_{60}, *Phys. Rev. B: Condens. Matter Mater. Phys.*, 1995, **52**, 15534–15536.

15 S. Margadonna, J. Arvanitidis, K. Papagelis and K. Prassides, Negative thermal expansion in the mixed valence ytterbium fulleride, $Yb_{2.75}C_{60}$, *Chem. Mater.*, 2005, **17**, 4474–4478.

16 M. Akada, T. Hirai, J. Takeuchi, T. Yamamoto, R. Kumashiro and K. Tanigaki, Superconducting phase sequence in R_xC_{60} fullerides (R = Sm and Yb), *Phys. Rev. B: Condens. Matter Mater. Phys.*, 2006, **73**, 094509.

17 A. Jayaraman, V. Narayanamurti, E. Bucher and R. G. Maines, Continuous and discontinuous semiconductor-metal transition in samarium monochalcogenides under pressure, *Phys. Rev. Lett.*, 1970, **25**, 1430–1433.

18 D. Malterre, M. Grioni and Y. Baer, Recent developments in high-energy spectroscopies of Kondo systems, *Adv. Phys.*, 1996, **45**, 299–348.

19 J. Arvanitidis, K. Papagelis, S. Margadonna and K. Prassides, Lattice collapse in mixed-valence samarium fulleride $Sm_{2.75}C_{60}$ at high pressure, *Dalton Trans.*, 2004, 3144–3146.

20 S. M. Souliou, J. Arvanitidis, D. Christofilos, K. Papagelis, S. Ves, G. A. Kourouklis, K. Prassides, Y. Iwasa and K. Syassen, High-pressure Raman study of the $Sm_{2.75}C_{60}$ fulleride, *High-Pressure Res.*, 2011, **31**, 13–17.

21 A. Jayaraman, P. Dernier and L. D. Longinotti, Study of the valence transition in SmS induced by alloying, temperature, and pressure, *Phys. Rev. B: Condens. Matter Mater. Phys.*, 1975, **11**, 2783–2794; A. Jayaraman and R. G. Maines, Study of the valence transition in Eu-, Yb-, and Ca-substituted SmS under high pressure and some comments on other substitutions, *Phys. Rev. B: Condens. Matter Mater. Phys.*, 1979, **19**, 4154–4161.

22 K. Takenaka, Progress of research in negative thermal expansion materials: paradigm shift in the control of thermal expansion, *Front. Chem.*, 2018, **6**, 267.

23 Y. Yokoyama, H. Hasegawa, Y. Mizuno, D. Asai, Y. Okamoto, H. S. Suzuki, K. Takehana, Y. Imanaka and K. Takenaka, Effects of Y substitution on the electronic structure and charge dynamics of SmS, *Phys. Rev. B*, 2019, **100**, 245143.

24 D. G. Mazzone, M. Dzero, AM. M. Abeykoon, H. Yamaoka, H. Ishii, N. Hiraoka, J.-P. Rueff, J. M. Ablett, K. Imura, H. S. Suzuki, J. N. Hancock and I. Jarrige, Kondo-induced giant isotropic negative thermal expansion, *Phys. Rev. Lett.*, 2020, **124**, 125701.

25 N. Yoshikane, T. Nakagawa, K. Matsui, H. Yamaoka, N. Hiraoka, H. Ishii, J. Arvanitidis and K. Prassides, Chemical tuning of samarium valence in mixed valence $(Sm_{1-x}Ca_x)_{2.75}C_{60}$ fullerides, *J. Phys. Chem. Solids*, 2020, under review.

26 M. B. Maple and D. Wohlleben, Nonmagnetic 4f shell in the high-pressure phase of SmS, *Phys. Rev. Lett.*, 1971, **27**, 511–515.

27 J.-P. Rueff and A. Shukla, Inelastic X-ray scattering by electronic excitations under high pressure, *Rev. Mod. Phys.*,

2010, **82**, 847–896; H. Yamaoka, Pressure dependence of the electronic structure of 4f and 3d electron systems studied by X-ray emission spectroscopy, *High-Pressure Res.*, 2016, **36**, 262–274.

28 G. Materlik, J. E. Muller and J. W. Wilkins, L-edge absorption spectra of the rare earths: assessment of the single-particle picture, *Phys. Rev. Lett.*, 1983, **50**, 267–270; E. Beaurepaire, J. P. Kappler and G. Krill, X-ray-absorption near-edge structure study in mixed-valent samarium systems, *Phys. Rev. B: Condens. Matter Mater. Phys.*, 1990, **41**, 6768–6776.

29 I. Jarrige, H. Yamaoka, J.-P. Rueff, J.-F. Lin, M. Taguchi, N. Hiraoka, H. Ishii, K. D. Tsuei, K. Imura, T. Matsumura, A. Ochiai, H. S. Suzuki and A. Kotani, Unified understanding of the valence transition in the rare-earth monochalcogenides under pressure, *Phys. Rev. B: Condens. Matter Mater. Phys.*, 2013, **87**, 115107.

30 P. P. Deen, D. Braithwaite, N. Kernavanois, L. Paolasini, S. Raymond, A. Barla, G. Lapertot and J. P. Sanchez, Structural and electronic transitions in the low-temperature, high-pressure phase of SmS, *Phys. Rev. B: Condens. Matter Mater. Phys.*, 2005, **71**, 245118.

31 A. Barla, J. P. Sanchez, Y. Haga, G. Lapertot, B. P. Doyle, O. Leupold, R. Rüffer, M. M. Abd-Elmeguid, R. Lengsdorf and J. Flouquet, Pressure-induced magnetic order in golden SmS, *Phys. Rev. Lett.*, 2004, **92**, 066401; A. Barla, J.-P. Sanchez, J. Derr, B. Salce, G. Lapertot, J. Flouquet, B. P. Doyle, O. Leupold, R. Rüffer, M. M. Abd-Elmeguid and R. Lengsdorf, Valence and magnetic instabilities in Sm compounds at high pressures, *J. Phys.: Condens. Matter*, 2005, **17**, S837–S848.

32 H. Yamaoka, I. Jarrige, N. Tsujii, M. Imai, J.-F. Lin, M. Matsunami, R. Eguchi, M. Arita, K. Shimada, H. Namatame, M. Taniguchi, M. Taguchi, Y. Senba, H. Ohashi, N. Hiraoka, H. Ishii and K.-D. Tsuei, Electronic structure of $YbGa_{1.15}Si_{0.85}$ and $YbGa_xGe_{2-x}$ probed by resonant X-ray emission and photoelectron spectroscopies, *Phys. Rev. B: Condens. Matter Mater. Phys.*, 2011, **83**, 104525.

33 K. Yokogawa, K. Murata, H. Yoshin and S. Aoyama, Solidification of high-pressure medium Daphne 7373, *Jpn. J. Appl. Phys.*, 2007, **46**, 3636–3639.

34 H. K. Mao, J. Xu and P. M. Bell, Calibration of the ruby pressure gauge to 800 kbar under quasi-hydrostatic conditions, *J. Geophys. Res.*, 1986, **91**, 4673–4676.

